THE AMERICAN SOCIETY OF MECHANICAL ENGINEERS
345 E. 47th St., New York, N.Y. 10017

97-GT-99

ENGINE REPRESENTATIVE DISCHARGE COEFFICIENTS MEASURED IN AN ANNULAR NOZZLE GUIDE VANE CASCADE

D.A. Rowbury and M.L.G. Oldfield
Department of Engineering Science, University of Oxford, Oxford, UK

G.D. Lock
School of Mechanical Engineering, University of Bath, Bath, UK

ABSTRACT

This paper discusses measurements of the discharge coefficients of gas turbine nozzle guide vane film cooling holes under fully engine representative conditions. These unique experiments were carried out in a large scale annular blowdown cascade which models the three-dimensional external flow patterns found in modern aero-engines, including all secondary flow phenomena. Furthermore, the coolant system design allows the coolant-to-mainstream density ratio and blowing parameter to be matched to engine values, although they can be independently varied.

The results confirm that the discharge coefficients of film cooling holes are significantly altered by external crossflow. The discharge coefficient is usually reduced by external crossflow, but under certain external flow conditions it can be increased over the non-crossflow case. This previously unhighlighted phenomenon has been termed 'the crossover effect', and, although an initially surprising result, is of importance to aero-engine designers as taking account of it should lead to improved predictions of coolant consumption. As a consequence, more uniform blade cooling should be achieved and, in turn, the attainment of greater component durability will be possible.

1 NOMENCLATURE

1.1 Symbols

A	area
a	local speed of sound
B	coolant-to-mainstream blowing ratio $= \frac{\rho_{ca} u_{ca}}{\rho_m u_m}$
C_d	discharge coefficient $= \frac{\dot{m}_{actual}}{\dot{m}_{ideal}}$
d	diameter
l	hole length
$\dot{m}$	mass flow rate
M	Mach number
p	pressure
PR	pressure ratio across hole $= \frac{p_{oc}}{p_m}$
R	gas constant
Re	Reynolds number
T	temperature
u	velocity
α	angle of orientation
γ	ratio of specific heats
ρ	density
θ	angle of inclination

1.2 Subscripts

c	coolant
ca	air coolant
cf	foreign gas coolant
m	mainstream
o	total

2 INTRODUCTION

Blade film cooling permits an increase in turbine entry temperature by reducing the mainstream-to-blade heat transfer, which, in turn, results in a higher power output and increased turbine efficiency. This is offset by decreased output due to the coolant bypassing certain engine stages - thus passing through the remaining turbines at a lower temperature than it otherwise would do - and losing total pressure as it is ducted to the blade. Furthermore, the process of mixing the coolant with the mainstream air after ejection leads to a reduction in aerodynamic efficiency. Consequently, successful implementation of a cooling system involves careful design in order to achieve effective cooling (leading to maximum turbine entry temperature) without leading to a dramatic performance penalty.

A film cooling system is designed to supply the mass flow rate of coolant needed to produce a uniform blade temperature. Failing to do so will result in thermal stresses within the blade and,

Presented at the International Gas Turbine & Aeroengine Congress & Exhibition
Orlando, Florida — June 2–June 5, 1997

consequently, a reduced blade life. For a first stage nozzle guide vane (NGV), the coolant-to-mainstream pressure ratio is usually set by the compressor exit pressure, so the design problem hinges on correct hole sizing in order to provide the requisite coolant flow. This requires reliable discharge coefficient, C_d, data covering the particular geometry and flow.

It is understood that the engine designer specifies a hole area and C_d and then lets an iterative flow solver calculate the necessary film parameters for the boundary layer program to satisfy the required output heat flux. Ideally the designer would be looking to specify an external heat flux/film distribution and let the program calculate what mass flow is required. However, the designer has no way of automatically accounting for the effect of external crossflow - he has a correlation for internal crossflow - and so this work will be used to improve the estimate of C_d, and hence film mass flow, that is fed into the boundary layer code.

The C_d depends on both the local geometry and the flow conditions upstream and downstream of the hole. Hole geometries are chosen such that cooling effectiveness is maximised, with inclined holes often being used as higher effectiveness levels are achieved for shallow injection angles than for normal injection (see, for example, Sasaki et al., 1976, or Foster and Lampard, 1980). Furthermore, 'flared' or 'fanned' holes are often used in film cooling arrays as they reduce the momentum of the jet at exit, thereby improving the film cooling performance further (Hay and Lampard, 1995).

Obtaining Discharge Coefficients

The measurement of film-cooling hole discharge coefficients is a subject widely reported in the literature, although there is a general lack of data gathered in a true engine representative environment. There is a need for research of this nature - especially under engine representative conditions - in order to validate and improve upon existing CFD codes and to aid the attainment of greater component durability. There are a number of methods for obtaining the C_d of cooling holes, as discussed below. An excellent review of work in this field has been produced by Hay and Lampard (1996).

The first method for obtaining the C_d of cooling holes is by treating the inlet and outlet flows separately and then using a simple 'loss coefficient' type analysis (that includes mixing within the hole). The success of this method depends on the lack of significant interactions between the various elements, which generally limits its application to simple cases; the analysis of a plenum-fed, normal cooling hole by Andrews and Mkpadi (1983) is a good example for this case.

The second method involves modifying a basic hole C_d for the effects of geometric variations and the presence of crossflows. This technique has been found to accurately model individual effects - as demonstrated by Lichtarowicz et al. (1965), Rogers and Hersh (1975), Tillman and Jen (1984), Tay Chu et al. (1985), Hay et al. (1987), McGreehan and Schotsch (1988) and Hay et al. (1994a) - although it is, not surprisingly, less successful under more complex conditions.

The final method is by directly measuring the C_d of a hole having the correct geometry under the design flow conditions. This approach is, obviously, ideal for obtaining coolant hole discharge coefficients under design conditions, although it can be difficult to achieve this accurately. The work described in this paper uses this approach.

3 GEOMETRIC AND FLOW PARAMETERS

The NGV row being studied in the Cold Heat Transfer Tunnel (CHTT; Martinez-Botas et al., 1993) is representative of a first stage high pressure section of a modern aero-engine. The cooling geometry consists of fourteen rows of holes - 340 cooling holes in total, drilled in-house on a 5-axis numerically controlled machine - fed from one of two internal cavities, as illustrated in Figure 1. These cavities are independently supplied with coolant so as to maintain a coolant-to-mainstream total pressure ratio, p_{oc}/p_{om}, of 1.02. The 'forward' cavity supplies the twelve rows positioned around the leading edge and the early regions of the pressure and suction surfaces, while the 'rear' cavity feeds the two rows nearest the trailing edge on the pressure surface. The rows are approximately positioned along isopressure lines - implying there is no variation in the coolant total to mainstream static pressure ratio, $PR = p_{oc}/p_m$, across the holes within a row - and do not extend into the secondary flow regions on the suction surface.

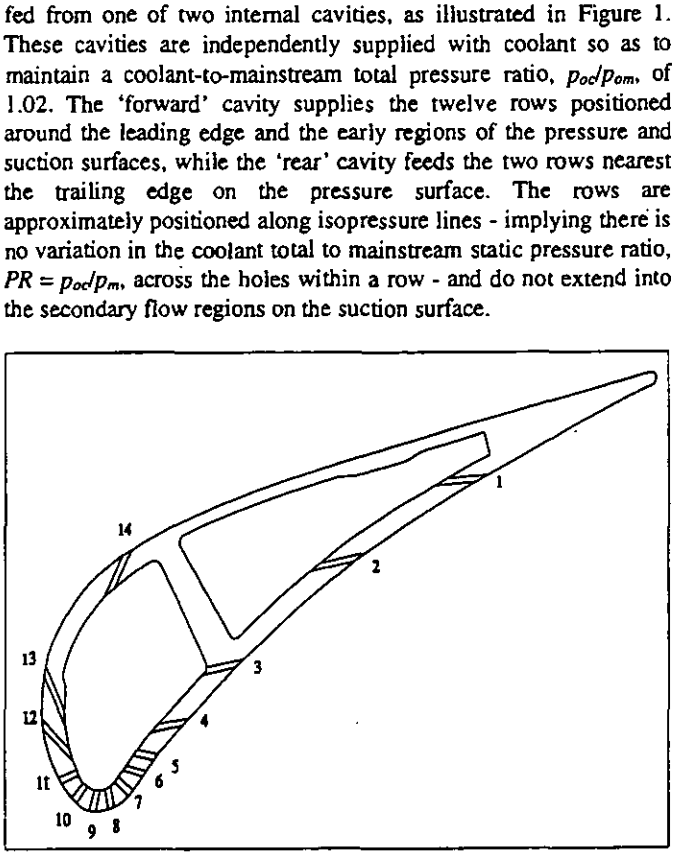

Figure 1 : Cross-Section of a CHTT NGV having the Full Film Cooling Geometry, Illustrating Row Positions

The cooling holes are all cylindrical, with sharp-edged inlets and length-to-diameter ratios greater than 3.5. As a consequence, the vena-contracta effect on the hole C_d will remain constant for any series of experiments on a single row, as it should be unaffected by the external flow.

It is worth noting that the range of flow conditions that are present amongst the different rows and holes is very diverse. For example, the mainstream (i.e. external) Mach number varies between 0.0 and 1.1 around the blade surface (the row Mach number, at 50% span, varying from 0.04 to 0.96). At the same time, the pressure ratio across the hole, PR, and the blowing (or mass flux) ratio, B, vary from 1.02 to 1.77 and 1.3 to 6.4 respectively. The hole geometries are equally variant, with the length-to-diameter ratio, l/d, being anywhere in the range $3.5 < l/d < 10.3$, and the two commonly defined hole angles (see, for example, Hay and Lampard, 1996) - the angles of inclination, θ, (the angle of the cooling hole

relative to the blade surface, $\theta = 90°$ being perpendicular to the surface) and orientation, α, (the angle, in plan view, of the cooling hole relative to the external streamline, $\alpha = 0°$ being parallel to the streamline) - varying significantly, namely in the ranges $20° < \theta < 90°$ and $0° < \alpha < 60°$. Generally, the holes around the leading edge region have steep inclination angles (i.e. $\theta \sim 90°$) and large angles of orientation ($\alpha \sim 60°$), whereas away from this region the holes have shallow inclination angles ($20° < \theta < 60°$) and very small angles of orientation ($\alpha \sim 0°$). This angling of the holes is present to aid the internal cooling, by having the coolant in contact with the blade material for longer as it passes from the cavity to the mainstream, and to maximise cooling effectiveness.

By testing an actual engine blade cooling configuration, rather than a simplified model where a single parameter could be varied at any one time, l/d, B, θ, α and M all vary between the rows, making it difficult to draw conclusions on individual trends from the results. However, it is hoped that this work will highlight areas where fundamental research should concentrate in the future.

4 TEST FACILITY

The experimental work summarised in this paper was carried out in the CHTT in Oxford. The CHTT is an annular cascade of 36 NGVs at 1.4 times larger than engine size, resulting in good spatial resolution on all measurements taken. Table 1 gives the salient NGV dimensions, whilst the rig is shown schematically in Figure 2.

Mid-span axial chord	0.0664 m
Mean pitch at exit	0.09718 m
Span at exit	0.08076 m
Turning angle	73°
Throat area	0.08056 m^2
Mean blade diameter	1.113 m
mainstream turbulence level (at NGV inlet)	13%

Table 1 : CHTT NGV Details

The CHTT is a short duration (typically 5-7 seconds), transonic test facility, which not only provides engine representative Reynolds and Mach numbers, but also, being an annular cascade of NGV blades, models the three-dimensional flow patterns found in modern aero-engines, including all secondary flow phenomena. Moreover, the coolant system design allows the engine density ratio, ρ_c/ρ_m, and blowing parameter, $\rho_c u_c/\rho_m u_m$, to be matched to and varied about actual engine design values.

All 36 blades in the annulus have the same surface geometry. The test blade and the two adjacent blades have the full film cooling configuration (Figure 3), whilst the remaining 33 NGVs have only 4 rows of cooling holes, fed from a single internal cavity. Those blades having the simplified cooling geometry - 'dummy' blades - are present to provide periodicity of flow around the cascade, by matching aerodynamic blockage, whilst providing a substantial saving in manufacturing costs.

The coolant (either air or foreign gas, the latter of which is a dense gas used to simulate the lower coolant temperature; see Section 5) is supplied to blades having the full cooling geometry from high pressure bottles (Figure 2), with the flow being regulated

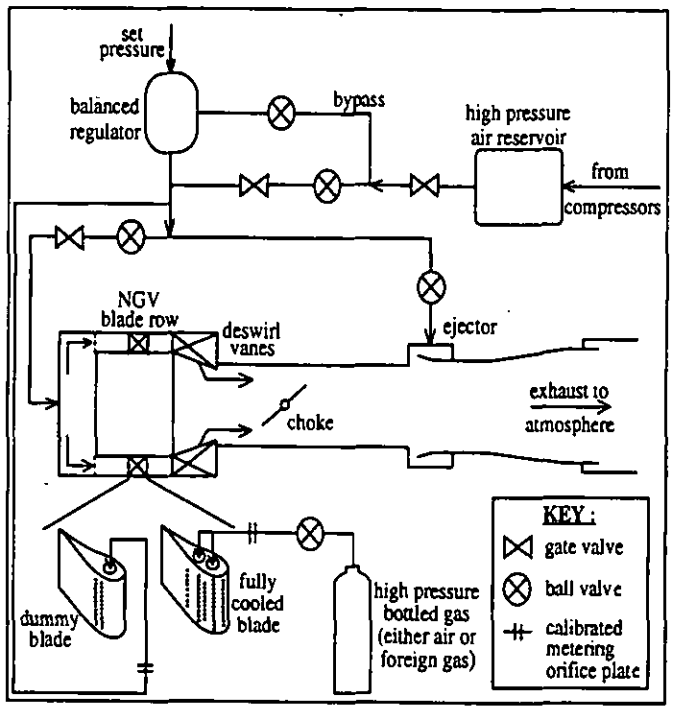

Figure 2 : Schematic Diagram of the CHTT

by means of choked calibrated metering orifice plates. Having passed through the orifice plate, the coolant flows into the internal cavity of the blade where it stagnates before flowing out through the (open) film cooling holes and mixing with the mainstream flow. The coolant-to-mainstream pressure ratio can be varied, whilst the use of air, foreign gas or a mixture of these as coolant permits data to be collected for coolant-to-mainstream density ratios in the range 1 to 1.77.

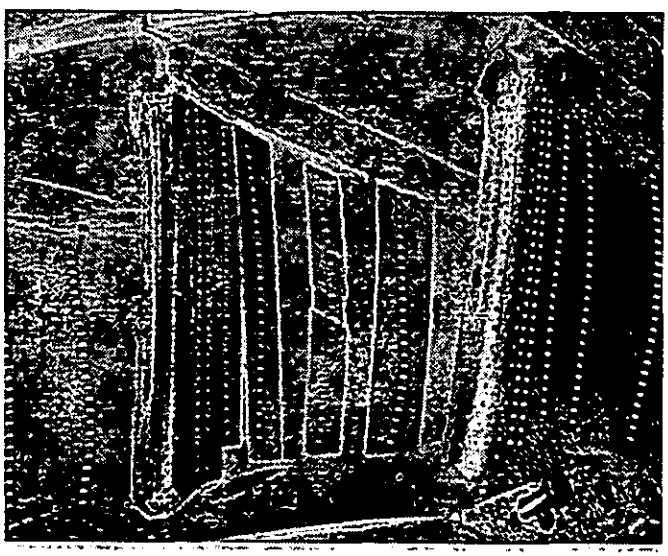

Figure 3 : CHTT NGV having the Full Film Cooling Geometry. The Centre Blade has All but 3 Holes of Row 6 Sealed with Kapton Tape

5 THEORY AND EXPERIMENTAL TECHNIQUE

5.1 Flow Measurement

The discharge coefficient of a film cooling hole is defined as the ratio of the measured (i.e. actual) to the ideal mass flow rate of coolant, $\frac{\dot{m}_{actual}}{\dot{m}_{ideal}}$. If the static pressure at the exit from the holes, p_m, and the cavity (upstream) total pressure and temperature, p_{oc} and T_{oc}, are known, then the isentropic flow equations can be used to determine the ideal mass flow rate, giving :

$$\dot{m}_{ideal} = A.\left(\frac{p_m}{p_{oc}}\right)^{\frac{1}{\gamma}}.\frac{p_{oc}}{\sqrt{RT_{oc}}}.\sqrt{\frac{2\gamma}{\gamma-1}.\left[1-\left(\frac{p_m}{p_{oc}}\right)^{\frac{\gamma-1}{\gamma}}\right]} \quad , \qquad (1)$$

for unchoked flow, and :

$$\dot{m}_{ideal} = \left(\frac{2}{\gamma+1}\right)^{\frac{\gamma+1}{2(\gamma-1)}}.A.p_{oc}.\sqrt{\frac{\gamma}{RT_{oc}}} \qquad (2)$$

for choked flow. It should be realised that in all calculations of $\dot{m}_{ideal}$ the cross-sectional area of the holes was used.

The isentropic Mach number distribution over the blade surface is known from experiment (Section 5.4) and has excellent run-to-run repeatability. The static pressure on the blade surface is then determined from the total pressure upstream of the cascade, p_{om}, and M. Consequently, $\dot{m}_{ideal}$ can be determined from p_{om}, p_{oc}, T_{oc} and M.

5.2 Simulation of Engine Coolant

A 'foreign gas' coolant is employed in order to match the engine coolant-to-mainstream density ratio in the fully film cooled (test) blades. It was demonstrated by Teekaram et al. (1989) that simulation of this density ratio is possible using a foreign injection gas. For optimum aerodynamic simulation, the foreign gas should have a ratio of specific heats equal to that of air (γ = 1.4) but a higher density than air, at the same temperature, in order to simulate the cold cooling gas. The gas chosen for such a role is a mixture of sulphur hexafluoride (SF_6; 30.2% by weight) and argon (Ar; 69.8% by weight), an inert gas with a low toxicity rating.

However, when employing a foreign injection gas it is difficult to simultaneously match blockage at the mainstream throat, the engine pressure ratios and the scaled engine mass flow rates. It was decided that the blockage and pressure ratios were the important parameters, and that these should be matched if possible.

Matching blockage between the engine and CHTT coolant flows implies that, for a given mainstream flow, the product ($\dot{m}\sqrt{RT}/M$) should be the same for both flows. However, matching $\dot{m}\sqrt{RT}$ and the Mach number, M, results in the coolant momentum flux, $\dot{m}_c u_c = \dot{m}_c.M_c a_c = \dot{m}_c.M_c\sqrt{\gamma R_c T_c}$, also being conserved. As a result, the total and static pressures are the same, thereby achieving similarity of the key parameters.

A similar argument can be used to match the different coolant flows within the CHTT (i.e. air or foreign gas coolant). Applying the above criteria, assuming the coolants are at the same total temperature, air and foreign gas cooling are correctly modelled if :

$$\dot{m}_{ca} = \dot{m}_{cf}\sqrt{\frac{R_{cf}}{R_{ca}}} \quad . \qquad (3)$$

Consequently, blades having the full cooling geometry are cooled with foreign gas when matching the engine mainstream-to-coolant density ratio and air when investigating the effect of altering this density ratio. At the same time, the dummy blades are always air cooled.

When the test blades are cooled with foreign gas, all of the major flow parameters except the scaled engine mass flow rates are then simultaneously matched to the engine condition (i.e. total and static pressure ratios, blockage at the mainstream throat, density ratios, mainstream Reynolds number and the local Mach numbers in the coolant and mainstream are all matched).

It should be realised that by simulating the density ratio through the use of a foreign injection gas (i.e. low R), the ratio of RT is matched and, therefore, so is the ratio of speed of sound. In turn, the engine coolant-to-mainstream velocity ratio, u_c/u_m, is matched, varying between 0.75 and 3.80.

Although the mainstream Reynolds number matches the engine value, it was not possible with an ambient temperature coolant to match the coolant Re_c based on hole exit diameter. The values of Re_c are similar for foreign gas or air coolant at ambient temperature (~21,000 and 17,000 respectively for Row 14 at the design PR), but are lower than the engine value (~59,000). However, the relative effect of external flow on C_d is almost independent of Re_c at these values (Andrews and Mkpadi, 1983, Tay Chu et al., 1985).

5.3 Experimental Technique

The two principal aspects to the establishment of a working experimental arrangement now become apparent.

Firstly, a set of orifice plates were accurately calibrated in order that known, controllable coolant mass flow rates could be provided. These were produced by feeding a flow of air through the choked orifice, whilst measuring the upstream total pressure and temperature (giving $\dot{m}_{ideal}$ from Eq. (2)), and on through a BS specified tube to a BS orifice plate, where measured pressures and temperatures, in conjunction with BS formulae, are used to calculate $\dot{m}_{actual}$. For further details on the calibration procedure see BS 1042 (British Standards Institution, 1981). The calibration was carried out against two differently sized British Standard plates (with BS orifice-to-pipe diameter ratios of 0.203 and 0.500), over the range of required orifice feed pressure, the double calibration providing evidence of the accuracy that is achieved using this method. Calibration accuracy of within +/- 1.0% is attainable, which results in a similar error in calculated C_d. This is within the error introduced due to uncertainty in the cooling hole diameter.

Orifice sizes were chosen such that flow could be provided, over a pressure range encompassing the design value, to any number of open holes from one to an entire cavity. As such, mass flow rates from 0.050 to 55.0 g s^{-1} were required, which, due to

limits on the range of supply pressure available, meant that a series of calibrated orifice plates from 0.32 to 3.80 mm in diameter were used. Due to the need for calibration over such a large mass flow range, two differently sized BS calibration rigs had to be employed.

Secondly, an effective method of selectively sealing-off holes had to be developed. This was achieved using Kapton sheet and 3M VHB (Very High Bond) adhesive tape (Figure 3). This novel usage of the Kapton allowed the application of relatively large cavity-to-external pressure ratios (up to ~3) without leakage, whilst minimising the aerodynamic interference (total thickness of only 40μm).

The effect of varying the density ratio, ρ_c/ρ_m, and the blowing rate, $\rho_c u_c/\rho_m u_m$, could then be investigated for any combination of open film cooling holes by changing the coolant used and the pressure ratio across the hole respectively. However, it should be noted that it was not possible to sweep through a range of blowing rates during the five seconds of tunnel operation due to the long settling times required at low coolant flow rates, and so steady state tests were always performed.

5.4 Pressure Measurement Accuracies

To provide a datum for studying the influence of external flow, the hole discharge coefficients were also measured without external flow. Figure 4 illustrates the good agreement in the experimentally determined discharge coefficients of different combinations (all, 14, 3 or a single hole) of open film cooling holes within a row when using four different metering orifices. This supports the earlier claims on the attainable accuracy when calibrating choked orifice plates and illustrates the consistency in the diameters of the machined cooling holes.

The agreement in calculated C_d between the different numbers of open holes also implies that any internal velocity is negligible as this would otherwise affect the discharge coefficient (Hay et al., 1994b). This is not surprising as the maximum internal crossflow (i.e. cavity) velocity, for all holes open within a row, is less than 10 m s^{-1} (i.e. $M_c < 0.03$). Obviously, the cavity velocity decreases proportionally with decreasing number of open cooling holes.

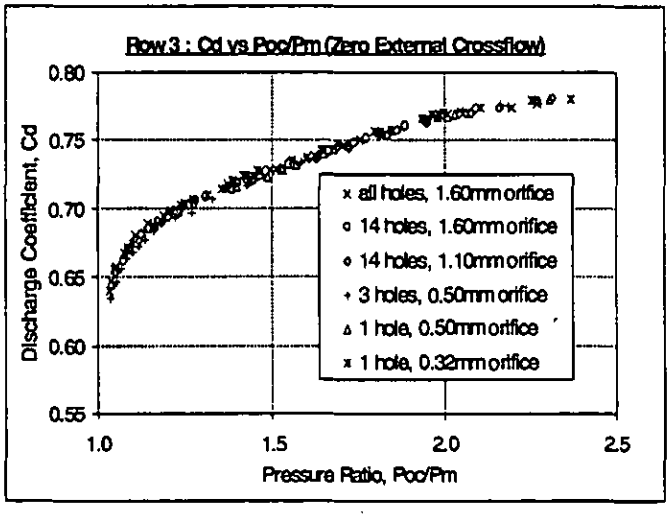

Figure 4 : Consistency in C_d Measurement Using Different Metering Orifice Plates

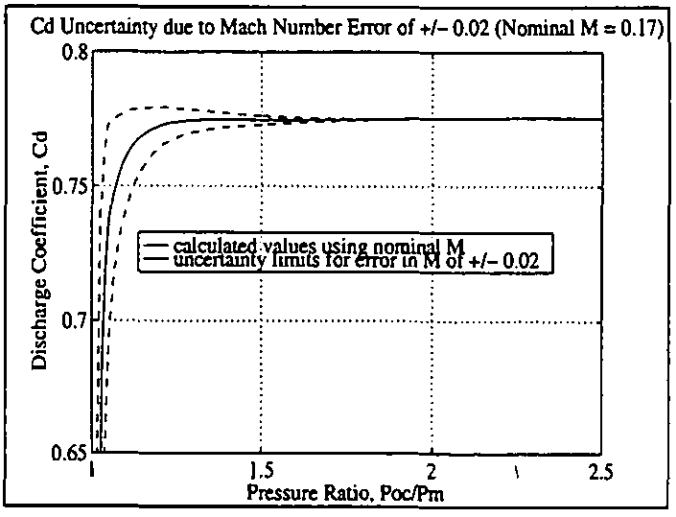

Figure 5 : Variation in C_d due to Error in Assumed External Mach Number

The importance of the external (i.e. blade surface) Mach number, M, should be realised as this both characterises the external flow and is used to calculate the external static pressure. Figure 5 illustrates the error in calculated C_d that can arise due to a nominal Mach number of 0.17 being in error by +/- 0.02. For a measured M, this corresponds to a static pressure measurement error of only 0.50%. As can be seen from Figure 5, this can lead to large uncertainties in C_d at low pressure ratios and so great care was taken to accurately determine the external Mach number.

Figure 6 shows the comparison between the engine designers' computational prediction of the blade surface Mach number at the row locations and the CHTT measurements, both with and without coolant flow, at 50% span. There are two main points of interest here. Firstly, it can be seen that the measurements were in good

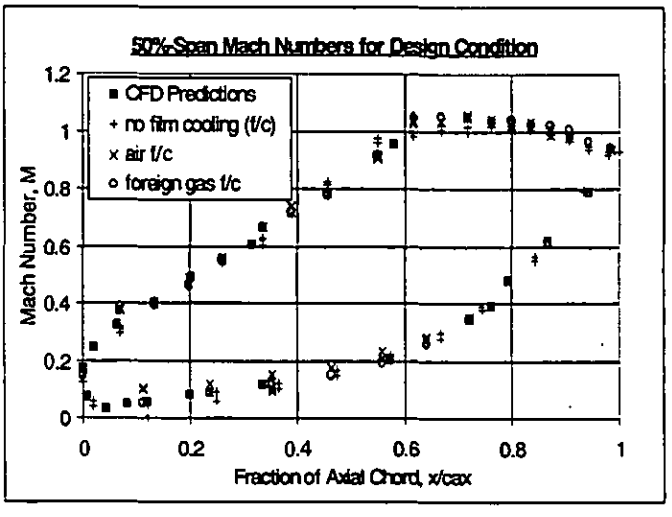

Figure 6 : Comparison Between Experimentally Determined Mach Number - With and Without Film Cooling (f/c) - and Designers' Prediction at the Cooling Hole Locations

agreement with the designers' prediction in all but the stagnation region, where it was difficult to obtain accurate measurements, and, secondly, it can be seen that the coolant flow appears to have very little affect on the Mach number distribution.

It was decided that the CFD prediction of Mach number at the row locations should be used as this would be more accurate than interpolating between the limited number of data points around the critical, leading edge region, where the measurements were relatively inaccurate. It was then assumed that the Mach number, and hence the hole exit static pressure, was constant for all holes within a row (i.e. the rows are located along isopressure lines). This assumption is justified by the fact that C_d vs PR data, with external crossflow, for all holes within a row agrees with that for the centre three holes within the row, implying a uniform mass flow distribution along a row of holes.

Just as the sensitivity to errors in Mach number increases in the low Mach number region, so does the sensitivity to errors in measured total pressures. Consequently, great care was needed in the measurement of these pressures (Rowbury et al., 1996).

6 RESULTS

Measurements with External Crossflow

The discharge coefficients of rows and groups of film cooling holes were experimentally determined over a range of cavity-to-external pressure ratios, incorporating the design case. Examples of data obtained are shown in Figures 7 to 11, illustrating three common features. Firstly, the mean C_d of the open holes when the flow is choked (i.e. $PR > 1.89$) is unaffected by whether or not there is crossflow at the hole exit. Secondly, that altering the coolant-to-mainstream density ratio - by changing from air to foreign gas coolant - has no effect on the hole C_d at the same PR. Finally, that there is generally a significant difference between the C_d of the holes with and without crossflow at typical engine pressure ratios. The authors consider the most important feature of the results to be this significant difference between the C_d with and without external crossflow.

It will also be noted that there is great similarity between the C_d vs PR curves without crossflow for Rows 3, 4, 9 and 14 (Figures 4/8, 9, 11 and 7 respectively), all of which have l/d ratios of about 7.0. This is both in terms of the form of the curve and in terms of the absolute C_d values. Of these, Row 9 has the smallest l/d ratio (6.1) but the highest C_d values. This trend is seen to continue when moving to Row 5 (Figure 10), which has a l/d ratio of 3.6 but a significantly higher C_d value at any given PR. It is well known that, for sharp edged holes, losses within the hole are dominated by inlet separation for small l/d ratios, but that frictional losses increase steadily with increasing l/d ratio (Andrews and Mkpadi, 1983). The values without crossflow closely agree with those predicted by Lichtarowicz et al. (1965), who concluded that for l/d ratios in the range 2-10, the C_d for choked flow would be given by :

$$C_d = 0.827 - 0.0085\, l/d \qquad (4)$$

Due to the complicated and varied geometries/flow conditions covered here, it is difficult to find suitable data in the published literature for direct comparison of the 'with crossflow' data (particularly for low M and large α). This lack of available data meant that it was beneficial to conduct our experiments on the specific engine geometry under engine representative conditions, i.e. in the CHTT. However, where applicable, reference is made to comparable data.

The data shown in Figure 7 (Row 14; $l/d = 7.0$, $\theta = 30°$ and $\alpha = 6°$) demonstrates what might be termed as the 'classical' behaviour (i.e. that oommonly highlighted in the literature), in that the discharge coefficient with crossflow is lower than the non-crossflow case for all pressure ratios. The data shows good agreement with an extrapolated version of sharp-edged hole data given by Hay et al. (1994a; $l/d = 6.0$, $\theta = 30°$, $\alpha = 0°$, $M_c = 0$ and $\underline{M_m = 0.45}$) and Hay et al. (1983; $l/d = 6.0$, $\theta = 30°$, $\alpha = 0°$, $M_c = 0$ and $\underline{M_m = 0.52}$).

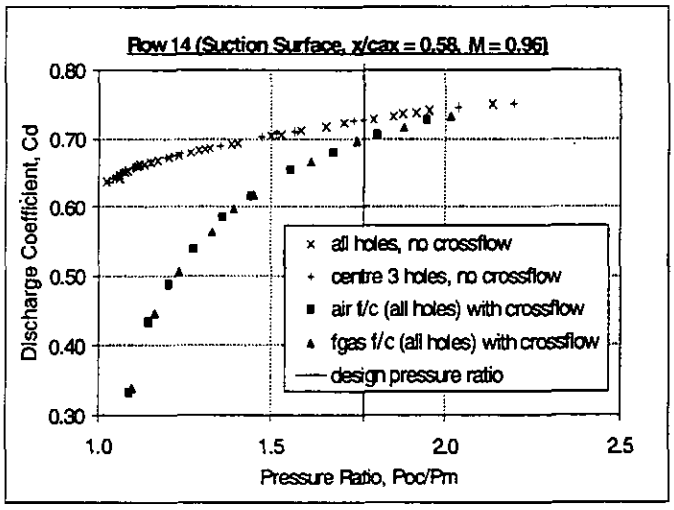

Figure 7 : C_d vs PR Data - With and Without External Crossflow - Illustrating 'Classical' Behaviour

In contrast, the data presented in Figure 8 (Row 3; $l/d = 7.5$, $\theta = 28°$ and $\alpha = 7°$) illustrates the case where, at the same pressure ratio, the with-crossflow data is initially lower than the non-crossflow data, but becomes higher than the non-crossflow case as the pressure ratio increases, and then tends to the same value at the critical pressure ratio ($PR = 1.89$), where the flow chokes. This is termed the 'crossover' phenomenon by the authors. The data is most comparable to the sharp edged hole data presented by Hay et al. (1983; $l/d = 6.0$, $\theta = 90°$, $\alpha = 0°$, $M_c = 0.3$ and $\underline{M_m = 0.11}$), which not only gives similar absolute values of C_d but also exhibits the crossover phenomenon. This is also the most suitable data that is available for comparison with that presented for Rows 4 and 5 (Figures 9 and 10 respectively).

It should be noted that there are a number of instances in the relevant publications where the data presented shows a tendency for the afore-mentioned crossover effect - see, for example, Rohde et al. (1969), Hay et al. (1983), Andrews and Sabersky (1990) or Hay et al. (1994a) - although the authors fail to discuss the phenomenon.

Figures 9 (Row 4; $l/d = 7.0$, $\theta = 30°$ and $\alpha = 7°$), 10 (Row 5; $l/d = 3.6$, $\theta = 58°$ and $\alpha = 0°$) and 11 (Row 9; $l/d = 6.1$, $\theta = 84°$ and $\alpha = 60°$) show further, increasingly pronounced examples of the crossover effect. The crossover is therefore seen to occur for rows on both the suction and pressure surfaces, with, to the best of the authors knowledge, none of the rows being located in regions of separation. Figure 10 demonstrates an example of the excellent

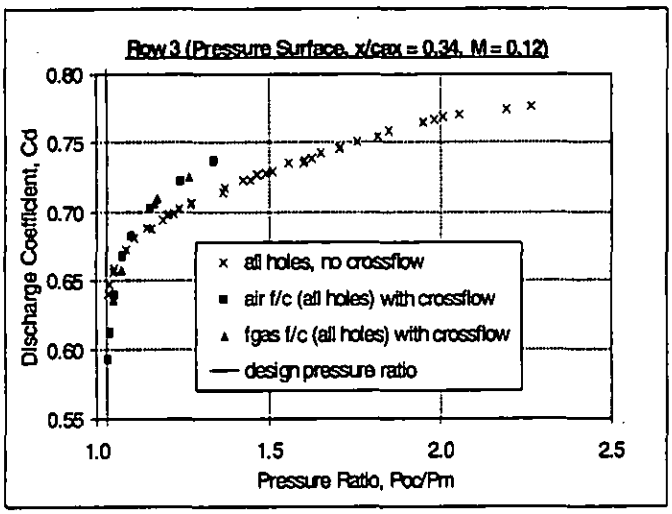

Figure 8 : C_d vs *PR* Data - With and Without External Crossflow - Illustrating the 'Crossover' Effect

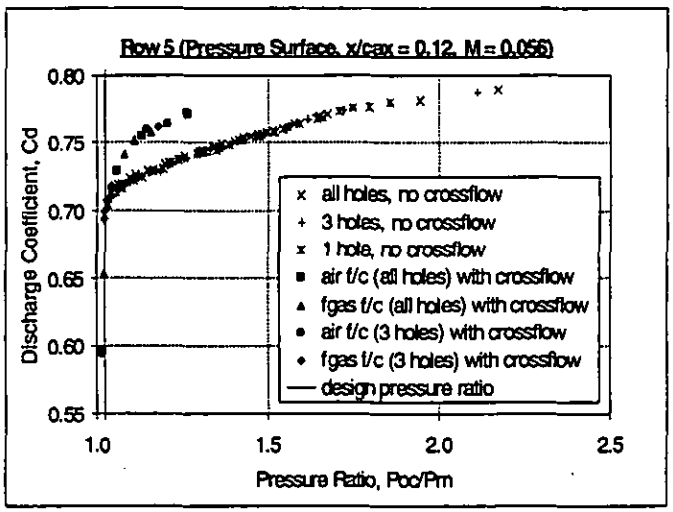

Figure 10 : C_d vs *PR* Data - With and Without External Crossflow - Illustrating the 'Crossover' Effect

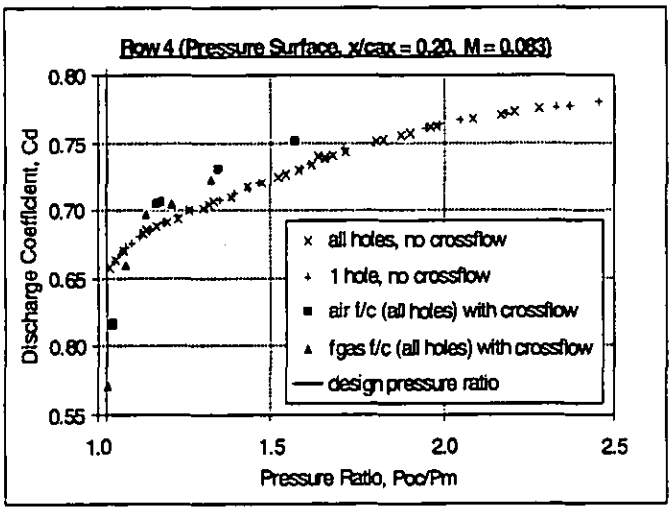

Figure 9 : C_d vs *PR* Data - With and Without External Crossflow - Illustrating the 'Crossover' Effect

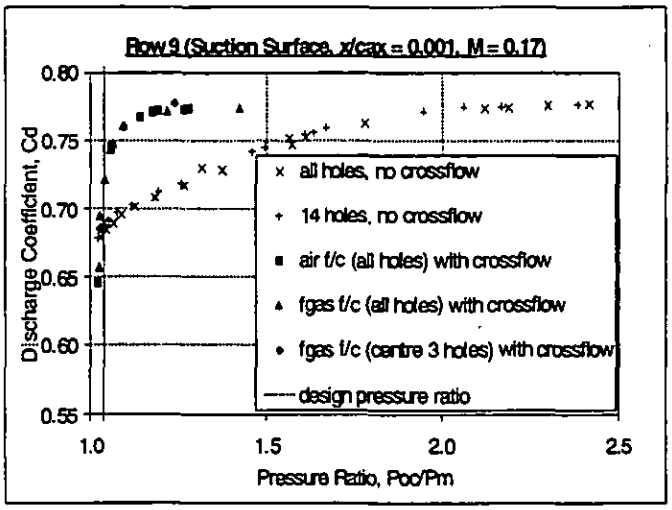

Figure 11 : C_d vs *PR* Data - With and Without External Crossflow - Illustrating the 'Crossover' Effect

agreement obtained between data collected for all holes and three holes within a row, providing evidence that the Mach number is constant along a row of holes and that the effect of internal velocity is negligible.

Of the thirteen rows of cooling holes studied, nine demonstrate some level of crossover, these being the rows having the lowest external Mach numbers ($M < 0.25$). However, as stated earlier, it is difficult to draw conclusions on trends present within the results because there are so many variables. However, we can say that the extent of the crossover depends on the external crossflow Mach number and the inclination and orientation of the hole to the flow.

7 DISCUSSION

It is the opinion of the authors that the crossover phenomenon results from a reduction in static pressure at the hole exit, p_m, due to a local acceleration of the mainstream flow. This acceleration is caused by blockage of the mainstream path by the exiting coolant flow, and results, effectively, in additional 'suction' on the coolant. This model would imply that the extent of the crossover would be greater for steeper inclination angles (i.e. $\theta \sim 90°$) and larger angles of orientation ($\alpha \sim 60°$), explaining why Row 9 (Figure 11) shows a more pronounced level of crossover than the other rows presented. This is supported by Hay et al. (1983) where the crossover is greater for normal holes ($\theta = 90°$) than for 30° inclined holes. However, such a model would suggest that crossover should occur to some extent for all geometries, which definitely is not the case. There are, therefore, two competing effects, the second being the 'pinching' of the coolant jet by the crossflow, a well documented effect to which Rogers and Hersh (1975) proposed the 'lid model'. This effect becomes progressively greater as the external crossflow Mach number, M_m, increases, possibly dominating for $M_m > \sim 0.25$. Consequently, the extent of the crossover depends on the external

crossflow Mach number and the inclination and orientation of the hole to the flow.

8 CONCLUSIONS

The discharge coefficients of cylindrical film cooling holes have been measured on a fully film cooled NGV blade in an annular cascade tunnel, under engine representative conditions, for two coolant-to-mainstream density ratios over a wide range of pressure ratio encompassing the design value. The discharge coefficients of film cooling holes are significantly affected by external crossflow - increased by up to 12% in the leading edge region and decreased by up to 12% away from it, at typical engine pressure ratios - the change depending on the geometric and flow conditions present. Although some of the results obtained could have been predicted from existing experimental data or empirical correlations, the effect of external flow has not been predicted accurately in all cases. Consequently, this experimental research is of interest to aero-engine designers as it should lead to modifications in their cooling hole C_d predictions.

The crossover phenomena is under further investigation.

9 ACKNOWLEDGEMENTS

This work has been carried out with the support of the Defence Research Agency (MoD & DTI) and Rolls-Royce Plc, the continuance of which is greatly appreciated by the authors, as is their permission to publish this work. The authors would also like to thank Professor T.V. Jones and Mr C.R.B. Day for their help and guidance, and Mr K. Walton and Mr T. Godfrey for their practical assistance.

REFERENCES

Andrews, G.E. and Mkpadi, M.C., 1983, "Full Coverage Discrete Hole Wall Cooling : Discharge Coefficients", ASME Paper No. 83-GT-79, International Gas Turbine Conference and Exhibit, Phoenix, Arizona, March 1983.

Andrews, K.A. and Sabersky, R.H., 1990, "Flow Through an Orifice From a Transverse Stream", ASME Paper No. 90-WA/FE-3, ASME Winter Annual Meeting, Dallas, Texas, November 1990.

British Standards Institution, 1981, "Methods of Measurement of Fluid Flow in Closed Conduits", BS 1042 : Section 1.1.

Foster, N.W. and Lampard, D., 1980, "The Flow and Film Cooling Effectiveness Following Injection through a Row of Holes", ASME Journal of Engineering for Power, Vol. 102, No. 3, pp. 584-588.

Hay, N., Henshall, S.E. and Manning, A., 1994b, "Discharge Coefficients of Holes Angled to the Flow Direction", ASME Journal of Turbomachinery, Vol. 116, pp. 92-96.

Hay, N., Khaldi, A. and Lampard, D., 1987, "Effect of Crossflows on the Discharge Coefficients of Film Cooling Holes with Rounded Entries or Exits", Proc. 2nd ASME-JSME Thermal Engineering Joint Conference, Honolulu, Hawaii, Vol. 3, pp. 369-374.

Hay, N. and Lampard, D., 1995, "The Discharge Coefficient of Flared Film Cooling Holes", ASME Paper No. 95-GT-15, International Gas Turbine and Aero-Engine Congress and Exposition, Houston, Texas, June 1995.

Hay, N. and Lampard, D., 1996, "Discharge Coefficient of Turbine Cooling Holes : A Review", ASME Paper No. 96-GT-492, International Gas Turbine and Aero-Engine Congress & Exhibition, Birmingham, UK, June 1996.

Hay, N., Lampard, D. and Benmansour, S., 1983, "Effects of Crossflows on the Discharge Coefficients of Film Cooling Holes", ASME Journal of Engineering for Power, Vol. 105, No. 2, pp. 243-248.

Hay, N., Lampard, D. and Khaldi, A., 1994a, "The Coefficient of Discharge of 30° Inclined Film Cooling Holes with Rounded Entries or Exits", ASME Paper No. 94-GT-180, International Gas Turbine and Aero-Engine Congress and Exposition, The Hague, Netherlands, June 1994.

Lichtarowicz, A., Duggins, R.K. and Markland, E., 1965, "Discharge Coefficients for Incompressible Non-Cavitating Flow Through Long Orifices", Journal of Mechanical Engineering Science, Vol. 7, No. 2, pp. 210-219.

Martinez-Botas, R.F., Main, A.J., Lock, G.D. and Jones, T.V., 1993, "A Cold Heat Transfer Tunnel for Gas Turbine Research on an Annular Cascade", ASME Paper No. 93-GT-248, International Gas Turbine and Aero-Engine Congress and Exposition, Cincinnati, Ohio, May 1993.

McGreehan, W.F. and Schotsch, M.J., 1988, "Flow Characteristics of Long Orifices with Rotation and Corner Radiusing", ASME Journal of Turbomachinery, Vol. 110, pp. 213-217.

Rohde, J.E., Richards, H.T. and Metger, G.W., 1969, "Discharge Coefficients for Thick Plate Orifices with Approach Flow Perpendicular and Inclined to the Orifice Axis, NASA-TN-D-5467.

Rogers, T. and Hersh, A.S., 1975, "The Effect of Grazing Flow on the Steady State Resistance of Square-Edged Orifices", American Institute of Aeronautics and Astronautics (AIAA) 2nd Aero-Acoustics Conference, Paper No. 75-493.

Rowbury, D.A., Oldfield, M.L.G. and Lock, G.D., 1996, "Discharge Coefficients of Nozzle Guide Vane Film Cooling Holes with Engine Representative External Flow", Proceedings of the 1996 Symposium on Measuring Techniques for Transonic and Supersonic Flow in Cascades and Turbomachines, Zurich, Sept. 1996.

Sasaki, M., Takahara, K., Sakata, K. and Kumagai, T., 1976, "Study on Film Cooling of Turbine Blades : Experiments on Film Cooling with Injection Through Holes near the Leading Edge", Bulletin of JSME, Vol. 19, No. 137, pp. 1344-1352.

Tay Chu, Brown, A. and Garrett, S., 1985, "Discharge Coefficients of Impingement and Film Cooling Holes", ASME Paper No. 85-GT-81, International Gas Turbine Conference and Exhibit, Houston, Texas, March 1985.

Teekaram, A.J.H., Forth, C.J.P. and Jones, T.V., 1989, "The Use of Foreign Gas to Simulate the Effects of Density Ratios in Film Cooling", Journal of Turbomachinery, Vol. 111, pp. 57-62.

Tillman, E.S. and Jen, H.F., 1984, "Cooling Airflow Studies at the Leading Edge of a Film-Cooled Airfoil", ASME Journal of Engineering for Gas Turbines and Power, Vol. 106, pp. 214-221.